THE JOURNAL OF PHYSICAL CHEMISTRY C

Article

pubs.acs.org/JPCC

Structural Dynamics of the Electrical Double Layer during Capacitive Charging/Discharging Processes

Masashi Nakamura,*[,†] Hiroto Kaminaga,[†] Osamu Endo,[‡] Hiroo Tajiri,[§] Osami Sakata,[∥] and Nagahiro Hoshi[†]

[†]Department of Applied Chemistry and Biotechnology, Graduate School of Engineering, Chiba University, Yayoi-cho 1-33, Inage-ku, Chiba 263-8522, Japan

[‡]Department of Organic and Polymer Materials Chemistry, Faculty of Engineering, Tokyo University of Agriculture and Technology, Naka-cho 2-24-16, Koganei, Tokyo 184-8588, Japan

[§]Research and Utilization Division, Japan Synchrotron Radiation Research Institute/SPring-8, Kouto 1-1-1, Sayo, Sayo-gun, Hyogo 679-5198, Japan

[∥]Synchrotron X-ray Station at SPring-8, National Institute for Materials Science, Kouto 1-1-1, Sayo-gun, Hyogo 679-5148, Japan

Supporting Information

ABSTRACT: Transitional structures of Cs^+ at the outer Helmholtz plane (OHP) have been determined using time-resolved X-ray diffraction during the double-layer charging/discharging on the Ag(100) electrode in CsBr solution. At the double-layer potential region at which c(2 × 2)-Br is formed on Ag(100), the transient current comprises two exponential terms with different time scales: a rapid and a slow one are due to the dielectric polarization of water molecules and the transfer of Cs^+, respectively. The slow term is composed of different dynamic processes of Cs^+ during charging and discharging. When the potential is stepped in the positive direction, the coverage of Cs^+ at the OHP decreases. In this step, the transient X-ray intensity at the (0 0 1) reflection, which is sensitive to the OHP structure, shows that Cs^+ is released from the OHP according to exponential function of time. The decay of transient intensity of X-ray has a time scale similar to that of the current transient measurement. On the other hand, the accumulation process of Cs^+ from the diffuse double layer to the OHP comprises two different kinetic processes after a potential step in the negative direction: a rapid one is the accumulation of Cs^+ near the outer layer, and a slow one is the structural stabilization of the Cs^+ layer.

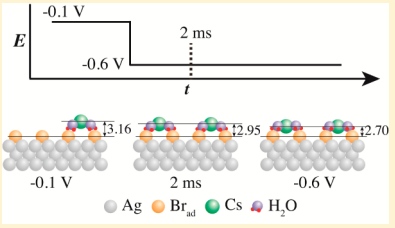

INTRODUCTION

Polarization of the electrode causes faradaic and capacitive currents through an electrochemical cell. The former is due to the chemical reaction accompanied by electron transfer between the electrode and the electrolyte. The latter is a "double-layer current" that originates from the accumulation of electrical charges and dielectric polarization.[1] In the case of aqueous electrolytes, the quantitative change in ionic species and reorientation of water molecules are caused in the electrical double layer (EDL). Migration of electrolyte ions in the EDL contributes to the double-layer current remarkably. However, there is no study on the correlation between the transient structure in the EDL and double-layer current.

The double-layer capacitors are based on the operating principle of the EDL and are widely used as electrical devices and batteries because of their high durability and rapid charging compared with chemical batteries. However, the energy density of the capacitor is lower than that of secondary batteries, such as the Li ion battery.[2] An interfacial structure that can store a large amount of charge is necessary for the development of high performance capacitors. Therefore, it is important to reveal the localization state of the charged species and the orientation of the dipole molecule in the EDL.

The structural behavior of an ionic species at the electrode/electrolyte interface is different from that in the bulk phase because of interactions with the surface and the strong electric field formed at the EDL. Although direct observation of nonspecifically adsorbed ions is restricted under electrochemical conditions, studies of X-ray diffraction recently revealed the structures of the ionic layer far from the electrode surface.[3−10] Ionic structures located at the outer Helmholtz plane (OHP) were determined with a constant electrode potential; the screening water layer is intercalated between the adsorbed ion layer and the OHP layer.[4,5] The coverage and distance of the Cs^+ ions from the surface depend on the electrode potential.[9] However, the correlation between the double-layer current and the double-layer structure is unknown. The transition structure after the potential step will be different from the static structure. The time-resolved X-ray diffraction (TRXD) method gives detailed structural information such as a structure of the rate-determining step during charging/

Received: July 13, 2014
Revised: September 2, 2014
Published: September 4, 2014

dx.doi.org/10.1021/jp506979p | J. Phys. Chem. C 2014, 118, 22136−22140

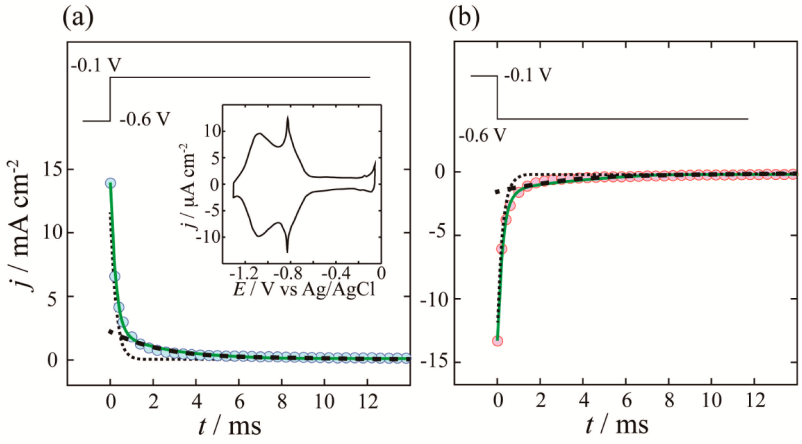

Figure 1. Current transients of Ag(100) in CsBr (a) from −0.6 to −0.1 V and (b) from −0.1 to −0.6 V. The green solid lines show the best fit to the experimental data (circles) using eq 2. The dotted and dashed lines are the first and the second terms of eq 2, which were obtained with k_1 = 11.6 mA cm^{-2}, k_2 = 2.2 mA cm^{-2}, τ_1 = 0.24 ms, and τ_2 = 2.3 ms for (a) and k_1 = −11.6 mA cm^{-2}, k_2 = −1.5 mA cm^{-2}, τ_1 = 0.24 ms, and τ_2 = 3.3 ms for (b). The inset shows the voltammogram of Ag(100) in CsBr. The scanning rate is 0.05 V s^{-1}.

discharging processes with high spatial and high time resolution.

The interface between the Ag(100) electrode and alkali metal bromide solution forms a typical EDL structure composed of the inner and the outer layers.[5] The inner layer has a stable c(2 × 2)-Br layer in the wide potential range, giving an appropriate structure for understanding the behavior of the OHP. Thus, the transition structures of cationic species at the OHP are investigated on Ag(100) using TRXD in this study. The transient structure of Cs^+ at the OHP on Ag(100) is determined: the coverage and distance from the surface depend on the time after the potential step. We also discuss the correlation between the transient current and OHP structure during the double-layer charging/discharging processes.

EXPERIMENTAL SECTION

The Ag(100) surface (Surface Preparation Laboratory) with a diameter of 10 mm was cut within 0.1°. The sample was etched in chromic acid solution followed by annealing to 700 K in H_2 + Ar using an induction heating furnace (AMBRELL). The annealed surface was protected with ultrapure water and transferred to the electrochemical cell. The drop cell, with the reference and counter electrodes immersed in the electrolyte droplet on the surface as shown in Figure S1 (Supporting Information),[11] was used for in situ TRXD and electrochemical measurement. The electrolyte solution of CsBr (Aldrich) was adjusted to pH 12.5 using CsOH (Aldrich) to confirm to previous experimental results.[5] The electrolyte concentration was 0.1 M CsBr + 0.05 M CsOH. The reference electrode was Ag/AgCl for all measurements. Electrochemical impedance spectroscopy (EIS) was measured using a frequency response analyzer (BioLogic SP-150) over the frequency range from 0.1 to 100 kHz with an a.c. amplitude of 5 mV. Fitting of impedance data was performed by using the equivalent circuit of the EDL.

TRXD measurements were performed with a multiaxis diffractometer at BL13XU (SPring-8) for surface and interface structure determination.[12] A rectangular potential wave between −0.1 and −0.6 V was applied to the Ag electrode with 10 Hz. Diffracted photons were counted by a multichannel scaler (Ortec) synchronized with the function generator for potential control. The diffraction intensity was accumulated over tens of thousands of cycles with a time resolution of 100 or 500 μs. The potential response of the electrochemical system, depending on the configuration of the counter and reference electrodes, was less than 10 μs for the potential pulses used in this study. The X-ray beam energies were 12.4 and 20 keV. A body-centered tetragonal coordinate system was used to describe the reciprocal vector as $Q = Ha^* + Kb^* + Lc^*$, where $a^* = b^* = 2\pi/a$, $c^* = \sqrt{2}\pi/a$, a = 2.889 Å, and L is the direction normal to the surface.[5] Structure refinement was performed using the least-squares method with the ANA−ROD program.[13]

RESULTS AND DISCUSSION

On Ag(100) in CsBr solution, a stable c(2 × 2) structure of adsorbed Br (Br_{ad}) is formed at a constant coverage of 0.5 above −0.6 V vs Ag/AgCl.[14,15] Figure 1 shows the current transients of Ag(100) in CsBr after the potential is stepped between −0.6 and −0.1 V where no faradaic current is found in the voltammogram, as shown in the inset of Figure 1(a). From the transient current between −0.6 and −0.1 V, the total charge density is estimated to be 13.5 μC cm^{-2}. Apparent exponential decay also suggests that the transient current is mainly caused by the capacitive component, i.e., the orientation change of the dipole solvent and the transfer of ionic species at the interface. The transient current including adsorption/desorption processes often deviates from a simple exponential function because of the nucleation and growth processes.[16,17]

The capacitive charge density can also be estimated from the double-layer capacitance of the EIS measurement. Figure 2 shows the potential-dependent differential capacitance of Ag(100) in CsBr obtained by fitting the equivalent RC circuit of the EDL. The capacitance curve is identical with the previous capacitance measurements recorded at E < −0.3 V.[18] The differential capacitance C in the electrical double layer is defined by eq 1.

$$C = \left(\frac{\partial q}{\partial E}\right) \quad (1)$$

where q is the charge density, and E is the electrode potential. From the shaded area in Figure 2, when the electrode potential changes between −0.1 and −0.6 V (i.e., ΔE = 0.5 V), the charge density is estimated to be Δq = 13 μC cm^{-2}. This value is

dx.doi.org/10.1021/jp506979p | J. Phys. Chem. C 2014, 118, 22136−22140

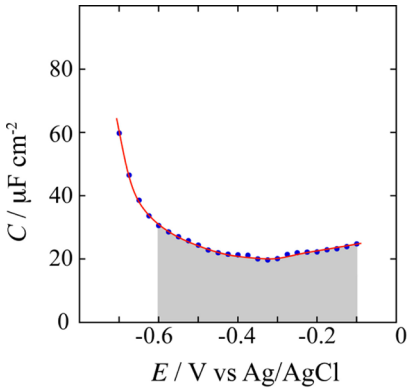

Figure 2. Potential dependence of differential capacitance of Ag(100) in 0.1 M CsBr. The impedance spectra were measured every 0.025 V.

similar to the total charge obtained by the current transient measurement, which supports that a non-faradaic process is dominant in this potential region.

A previous X-ray diffraction study revealed that the coverage of Cs^+ at the OHP changes by $\theta = 0.04$ between −0.1 and −0.6 V.[5] Since Cs^+ has a unit charge, the accumulated charge is 7.7 $\mu C\ cm^{-2}$ in the case of the coverage change of 0.04. This means that the charge of Cs^+ transfer accounts for about 60% of the total charge density estimated from the EIS (13 $\mu C\ cm^{-2}$) and the current transient (13.5 $\mu C\ cm^{-2}$). Although this ratio depends on electrolyte concentration, the major origin of the transient current is closely related to the transfer of Cs^+ to/from the OHP in this study.

In the absence of continuous mass−transport limitations and adsorption/desorption processes, the decay time of the transient current depends on electrolyte concentration (solution resistance) and double-layer capacitance, which is expressed by a single exponential function according to the classical RC network model. However, as shown in Figure 1, the transient currents j observed in CsBr fit well with the following two-term exponential equation

$$j = k_1 \exp(-t/\tau_1) + k_2 \exp(-t/\tau_2) \quad (2)$$

where k and τ are the amplitude and time constant, respectively. This result means that the double-layer current comprises two components with different time scales. Although the time constant ($\tau_1 = 0.24$ ms) of the first term is identical for charging and discharging, the time constant (τ_2) of the second term (3.3 ms) after stepping from −0.1 to −0.6 V is larger than that (2.3 ms) from −0.6 to −0.1 V. As discussed below, the transient current in the first and second terms can be assigned to the reorientation of water molecules and transfer of ionic species, respectively. The partial charge estimated from the second term of eq 2 accounts for 65% of the total charge estimated from eq 2. This percentage is similar to the ratio of charge density from the amount of Cs^+ change at the OHP. In this potential region, we reported that the coverage of Cs^+ increases monotonously with a decrease of the potential; i.e., an electrostatic charge of Cs^+ occurs at the OHP.[5] The longer time constant of the second term in the transient current from −0.1 to −0.6 V suggests the existence of a different kinetic state between charging and discharging processes of Cs^+. We tried to determine the transitional structure of Cs^+ by TRXD with the same cell geometry as that of the current transient.

In the specular crystal truncation rod (CTR) of Ag(100) in CsBr, potential-dependent changes are observed between −0.1 and −0.6 V (Figure 3). The bulge at $L = 1.0$ is due to the layered structure of Cs in the EDL.[5,9] Therefore, the reflection

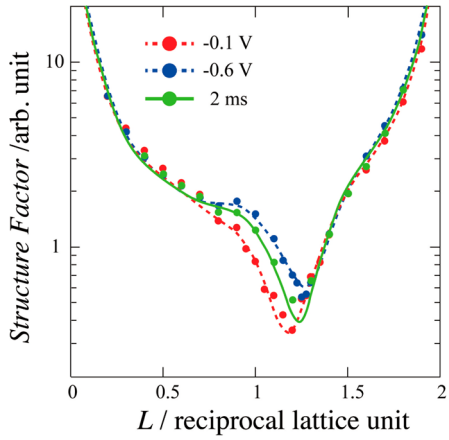

Figure 3. Time-resolved specular CTR of Ag(100) in CsBr at 2 ms after it was stepped from −0.1 to −0.6 V and at the static potentials of −0.1 and −0.6 V. The dashed and solid lines are structure factor calculated models.

around $L = 1$ is very sensitive to the coverage and distance from the surface of Cs^+ at the OHP. Figure 4(a) shows the rocking profile around the (0 0 1) position at −0.1 and −0.6 V. TRXD measurements were carried out by fixing the detector at the peak position of (0 0 1). Figures 4(b) and (c) show time-dependent X-ray diffraction intensities during the potential step between −0.1 and −0.6 V. We also measured TRXD at a half-maximum position in the rocking scan of the (0 0 1) position. Intensity decay at the half-maximum corresponds to that at the peak position (not shown here), indicating that dynamic intensity change is not caused by band broadening due to structural inhomogeneity; the homogeneous structural change occurs in the double layer.

For the transition from −0.6 to −0.1 V, the intensity at (0 0 1) decreases exponentially with time, as shown in Figure 4(b). The time constant of this intensity decay is 2.7 ms when fitted using a single exponential function, which is similar to that (2.3 ms) of the second term in the current transient measurement. This result indicates that the slow decay component of the anodic current from −0.6 to −0.1 V is closely related to the release of Cs^+ from the OHP in 0.15 M Cs^+ solution. Intensity decay in TRXD does not include the rapid decay component (0.24 ms) of the first term caused by the reorientation of water molecules. The electron density change by the reorientation of the light molecule is quite small relative to that by the transfer of Cs.

On the other hand, for the transition step from −0.1 to −0.6 V, the diffraction intensity change at (0 0 1) comprises two steps at the critical point of 2 ms: the first rapid step (<2 ms) and the second slow step (>2 ms), as shown in Figure 4(c). The increase in intensity is due to the accumulation of Cs^+ to the OHP.[5] The intensity decay in the accumulation process was fitted using a two-term exponential function. The time constants of the first and the second exponential components are 2.1 and 5.7 ms, respectively. The second term results in the slow kinetic process of Cs^+ in the EDL, which is not observed in the releasing process. The hysteresis behavior between releasing and accumulation of Cs^+ implies the existence of different transient structures.

dx.doi.org/10.1021/jp506979p | J. Phys. Chem. C 2014, 118, 22136−22140

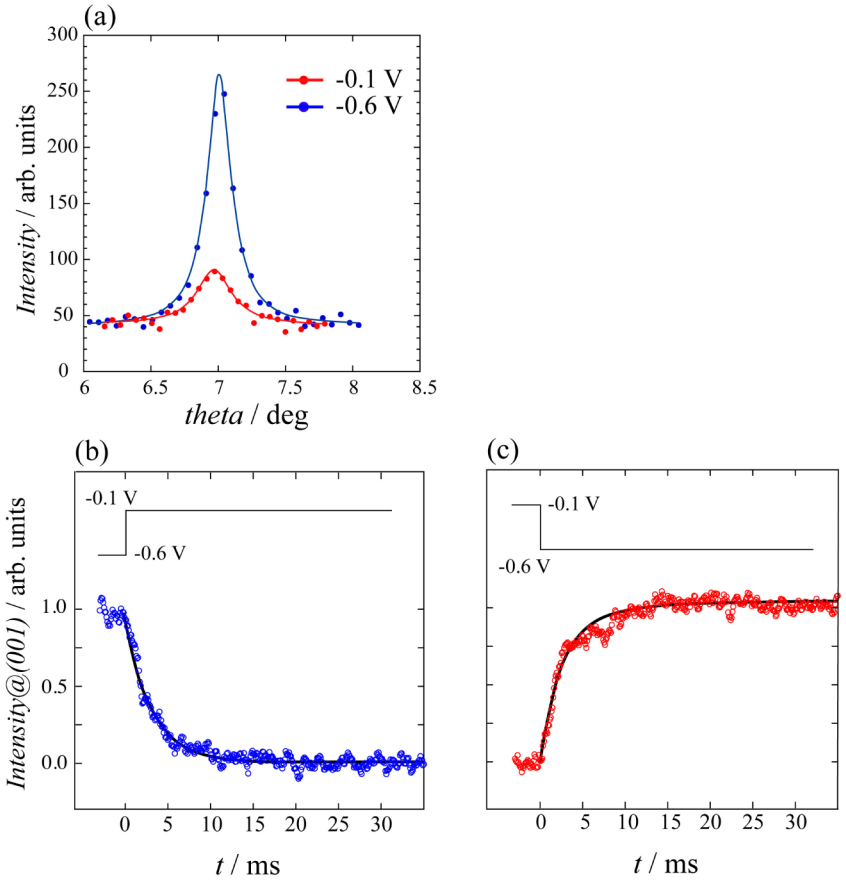

Figure 4. (a) X-ray diffraction profile of Ag(100) in 0.1 M CsBr measured by a rocking scan at (0 0 1) at −0.1 and −0.6 V. (b) and (c) Transient diffraction intensity at the peak position of the (0 0 1) reflection between −0.6 and −0.1 V. Time resolution is 100 μs. The solid lines show the best fit to the plots using (b) single and (c) two-term experimental functions.

We carried out time-resolved measurements at the peak positions along the CTR as shown in Figure S2 (Supporting Information) and determined the detailed structure at critical points (2 ms) to understand the slow kinetic process. Since the integrated intensity is proportional to the peak intensity without the band broadening as described above, the structure factor at each L position is estimated from the rate of change in the transient intensity based on the results at static potentials (−0.6 and −0.1 V). The solid line in Figure 3 shows the time-resolved CTR of the specular rod at 2 ms after it was stepped from −0.1 to −0.6 V. The CTR of $L < 2$ is shown because the dependence of the Cs structure appears around $L = 1.0$ clearly in this potential range.

We determined the interfacial structure at the static potential of −0.1 and −0.6 V first. The structural parameters, scale factor, Debye−Waller factor, and occupancy factor were optimized for Cs^+, Br_{ad}, and the first Ag layer. All of the parameters were refined simultaneously using a specular crystal truncation rod (CTR). Table 1 shows the coverage of Cs^+ and interlayer spacings. The structural parameters at −0.1 and −0.6 V are identical with those reported previously within experimental error.[5] Since the structural parameters for Br_{ad} and the Ag layer are constant in this double-layer region, the coverage and distance from the surface are optimized for Cs^+ at 2 ms after the potential step from −0.1 to −0.6 V. Compared with the results of the static potentials at −0.1 and −0.6 V, the slow process after 2 ms can be explained as follows. At −0.1 V, the coverage of Cs^+ and the distance from the surface are 0.06 and 3.16 Å, respectively, as shown in Figure 5(a). At 2 ms after the potential step to −0.6 V, the Cs coverage at the OHP increases from 0.06 to 0.11. This value is similar to that at −0.6 V. However, the distance from the surface is 2.95 Å, which does not reach the value of 2.70 Å at the static state at −0.6 V as shown in Figure 5(b) and (c). Structural analysis at 2 ms

Table 1. Coverage of Cs and the Layer Spacing d at 2 ms after Stepping from −0.1 to −0.6 V

	−0.1 V	−0.6 V	2 ms
θ_{Cs}[a]	0.06(1)	0.12(1)	0.11(1)
d_{Cs-Br} (Å)	3.16(10)	2.70(10)	2.95(10)
d_{Br-Ag} (Å)	1.95(3)	1.95(3)	1.95(3)

[a] θ_{Cs}: Cs coverage per Ag surface atom.

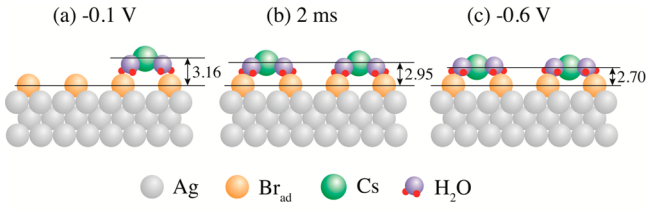

Figure 5. Schematic models of the transition structure of Ag(100) in CsBr. (a) and (c) Structures at static potentials at −0.1 and −0.6 V, respectively. (b)Sstructure at 2 ms during a potential step from −0.1 to −0.6 V.

dx.doi.org/10.1021/jp506979p | J. Phys. Chem. C 2014, 118, 22136−22140

indicates that the first step is related to the accumulation of Cs^+ from the diffuse double layer to the OHP, and the second step is related to the approach of the OHP layer to the surface. The slow kinetics for the second step is due to a blocking effect by the presence of hydration waters between the inner and outer layers. A previous density functional theory (DFT) calculation suggested that a screening water layer is intercalated between Br_{ad} and the outer Cs^+ layer, which is strongly oriented by the presence of charged species (Cs^+ and Br_{ad}). The oxygen of water is directed toward Cs^+, while hydrogen points toward Br_{ad} through hydrogen bonding. Thus, well-oriented intercalated water in the EDL is also reported on the Cu(100) electrode in KCl.[4] When Cs^+ approaches the surface through electrostatic interaction, Cs^+ pushes the oriented water layer aside. Therefore, the approach to the stable site of Cs^+ will be slower than the releasing process of Cs^+. The orientation of the screening water layer might be changed in accord with the change of electrode potential because of the interaction between the electric field and water dipole. It is also probable that the slow process is related to the surface phase transition of the Cs^+ layer. In the current transient, the time constant (τ_2) of the second term (3.3 ms), after stepping from −0.1 to −0.6 V, is longer than that (2.3 ms) for the step from −0.6 to −0.1 V. Metastable structures during the charging process of Cs^+ may delay the transient current from −0.1 to −0.6 V.

CONCLUSION

Transition structures of Cs at the OHP are determined using time-resolved X-ray diffraction in the double-layer region of Br adsorbed on the Ag(100) electrode. When the potential was stepped in the positive direction, Cs was released from the OHP at a similar time scale with the current transient measurement. For the negative potential step, the gathering process of Cs comprises two steps. The first step is the accumulation of Cs^+ near the outer layer, and the second one is structural stabilization of the Cs layer.

ASSOCIATED CONTENT

Supporting Information

Figures S1 and S2. This material is available free of charge via the Internet at http://pubs.acs.org.

AUTHOR INFORMATION

Corresponding Author

*E-mail: mnakamura@faculty.chiba-u.jp.

Notes

The authors declare no competing financial interest.

ACKNOWLEDGMENTS

TRXD measurements were supported by the Japan Synchrotron Radiation Research Institute (JASRI) under proposal numbers 2012B1126, 2013A1116, and 2013B1210. This work was supported by the Asahi Glass Foundation and Grant-in-Aid (KAKENHI) for Scientific Research (B) No. 24350001.

REFERENCES

(1) Conway, B. E. *Electrochemical Supercapactitors*; Springer: New York, 1999.

(2) Sharma, P.; Bhatti, T. S. A Review on Electrochemical Double-layer Capacitors. *Energy Convers. Manage.* **2010**, *51*, 2901−2912.

(3) Nakamura, M.; Sato, N.; Hoshi, N.; Sakata, O. Catalytically Active Structure of Bi Deposited Au(111) Electrode for Hydrogen Peroxide Reduction Reaction. *Langmuir* **2010**, *26*, 4590−4593.

(4) Keller, H.; Saracino, M.; Nguyen, H. M. T.; Broekmann, P. Templating the Near-surface Liquid Electrolyte: in Situ Surface X-ray Diffraction Study on Anion/cation Interactions at Electrified Interfaces. *Phys. Rev. B* **2010**, *82*, 245425.

(5) Nakamura, M.; Sato, N.; Hoshi, N.; Sakata, O. Outer Helmholtz Plane of the Electrical Double Layer Formed at the Solid-Liquid Interface. *ChemPhysChem* **2011**, *12*, 1430−1434.

(6) Strmcnik, D.; Vliet, D. F.; Chang, K. C.; Komanicky, V.; Kodama, K.; You, H.; Stamenkovic, V. R.; Markovic, N. M. Effects of Li^+, K^+, and Ba^{2+} Cations on the ORR at Model and High Surface area Pt and Au Surfaces in Alkaline Solutions. *J. Phys. Chem. Lett.* **2011**, *2*, 2733−2736.

(7) Lucas, C. A.; Thompson, P.; Grunder, Y.; Markovic, N. M. The Structure of the Electrochemical Double Layer: Ag(111) in Alkaline Electrolyte. *Electrochem. Commun.* **2011**, *13*, 1205−1208.

(8) Keller, H.; Saracino, M.; Nguyen, H. M. T.; Huynh, T. M. T.; Broekmann, P. Competitive Anion/water and Cation/water Interactions at Electrified Copper/electrolyte Interfaces Probed by in Situ X-ray Diffraction. *J. Phys. Chem. C* **2012**, *116*, 11068−11076.

(9) Nakamura, M.; Nakajima, Y.; Sato, N.; Hoshi, N.; Sakata, O. Structure of the Electrical Double Layer on Ag(100): Promotive Effect of Cationic Species on Br Adlayer Formation. *Phys. Rev. B* **2011**, *84*, 165433.

(10) Nakamura, M.; Nakajima, Y.; Hoshi, N.; Tajiri, H.; Sakata, O. Effect of Non-specifically Adsorbed Ions on the Surface Oxidation of Pt(111). *ChemPhysChem* **2013**, *14*, 2426−2431.

(11) Tamura, K.; Ocko, B. M.; Wang, J.; Adzic, R. R. Structure of Active Adlayers on Bimetallic Surfaces: Oxygen Reduction on Au(111) with Bi Adlayers. *J. Phys. Chem. B* **2002**, *106*, 3896−3901.

(12) Sakata, O.; Furukawa, Y.; Goto, S.; Mochizuki, T.; Uruga, T.; Takeshita, K.; Ohashi, H.; Ohta, T.; Matsushita, T.; Takahashi, S.; et al. Beamline for Surface and Interface Structures at SPring-8. *Surf. Rev. Lett.* **2003**, *10*, 543−547.

(13) Vlieg, E. ROD: A Program for Surface X-ray Crystallography. *J. Appl. Crystallogr.* **2000**, *33*, 401−405.

(14) Ocko, B. M.; Wang, J. X.; Wandlowski, T. Bromide Adsorption on Ag(001): Potential Induced Two-dimensional Ising Order-disorder Transition. *Phys. Rev. Lett.* **1997**, *79*, 1511−1514.

(15) Shimooka, T.; Inukai, J.; Itaya, K. Adlayer Structures of Cl and Br and Growth of Bulk AgBr Layers on Ag(100) Electrodes. *J. Electrochem. Soc.* **2002**, *149*, E19−E25.

(16) Holzle, M.; Retter, U.; Kolb, D. M. The Kinetics of Structural Changes in Cu Adlayers on Au(111). *J. Electroanal. Chem.* **1994**, *371*, 101−109.

(17) Wandlowski, T.; Wang, J. X.; Magnussen, O. M.; Ocko, B. M. Structural and Kinetic Aspects of Bromide Adsorption on Au(100). *J. Phys. Chem.* **1996**, *100*, 10277−10287.

(18) Wandlowski, Y.; Wang, J. X.; Ocko, B. M. Adsorption of Bromide at the Ag(100) Electrode Surface. *J. Electroanal. Chem.* **2001**, *500*, 418−434.